

Scientific paper

Thermodynamic Stability of the Dimeric Toxin CcdB

Mario Šimić, Gorazd Vesnaver and Jurij Lah*

University of Ljubljana, Faculty of Chemistry and Chemical Technology,
Aškerčeva 5, 1000 Ljubljana, Slovenia.

* Corresponding author: E-mail: jurij.lah@fkt.uni-lj.si
Phone: +386 1 2419 414; fax: +386 1 2419 425

Received: 29-10-2008

Dedicated to Professor Josef Barthel on the occasion of his 80th birthday

Abstract

The toxin-antitoxin module *ccd* located on *Escherichia coli* plasmid F encodes the antitoxin CcdA and the toxin CcdB. When not complexed with CcdA, CcdB attacks its cellular target gyrase and kills the cell by causing inhibition of both transcription and replication. At physiological conditions CcdB exists as a homodimer. Here we present a study of CcdB unfolding that is focused on the characterization of the structure-thermodynamics relationship needed for understanding the stability and function of CcdB at the molecular level. In this light, thermodynamic parameters of unfolding obtained by global analysis of urea-induced unfolding curves measured at various temperatures by circular dichroism spectroscopy were parsed into the contributions arising from the differences in intra- and inter-molecular interactions of CcdB in the folded dimeric and unfolded monomeric state. According to this parsing the unfolded monomers retain about 30% of the residual structure indicating that the urea-denatured state of CcdB is not a completely unfolded state.

Keywords: CcdB, toxin-antitoxin module, stability, structure, circular dichroism, programmed cell death

1. Introduction

The *ccd* operon located on *Escherichia coli* plasmid F is the toxin-antitoxin module¹ encoding the antitoxin CcdA and the toxin CcdB. CcdA inhibits the toxic activity of CcdB by forming a non-covalent CcdA:CcdB complex. CcdA and CcdB are co-expressed in plasmid F-bearing cells and their expression is autoregulated at the level of transcription by binding of CcdA:CcdB complex to the promoter DNA.^{2,3} Upon plasmid loss, CcdA is quickly degraded by Lon protease, releasing CcdB that by attacking the gyrase kills the cell.¹⁻⁴

Crystal structure of CcdB⁵ suggests that at physiological conditions it exists as a homodimer. Recent stability studies on CcdB have indicated that in buffer solution at physiological *pH* its thermal denaturation is irreversible if no additives that prevent its aggregation are present.^{6,7} On the other hand, it has been found recently that the chemical unfolding at relatively low temperatures is a reversible process accompanied by dissociation of the dimer.^{6,7} Although the reported analysis of the measured chemical un-

folding curves resulted in estimates of standard thermodynamic parameters of CcdB unfolding, these studies provided almost no information on the structure-thermodynamics relationship needed for understanding the stability and function of CcdB at the molecular level.

In this work we performed a global thermodynamic analysis of CcdB urea-induced unfolding curves measured by circular dichroism spectroscopy at various temperatures. An attempt was made to dissect the obtained thermodynamic stability into enthalpic and entropic contributions that can be further discussed in terms of structural features of CcdB native and denatured states.

2. Experimental

Materials. The preparation and purification of CcdB is described elsewhere.⁵ Its structure and the corresponding amino-acid sequence is given in Figure 1. Since CcdB is a homodimer in solution at non-denaturing conditions its molar concentration is expressed in mol_{dimer} L⁻¹. Solu-

tions of purified CcdB were dialyzed extensively against phosphate buffer (0.02 M Na-phosphate, 0.15 M NaCl, 0.001 M EDTA, pH = 7.5). All samples for the urea denaturation experiments were prepared by mixing 10 M urea and protein stock solution to a final urea concentration between 0 and 8 M. The pH of all solutions was checked and adjusted to 7.5 by addition of NaOH. Concentration of CcdB was determined spectrophotometrically from the absorbance measured at 280 nm in 6 M GdmHCl at 25 °C using extinction coefficients obtained using the method introduced by Gill and von Hippel⁸ (<http://www.expasy.ch>).

Circular dichroism spectroscopy (CD). CD measurements were performed with an AVIV Model 62A DS spectropolarimeter (Aviv Associates, USA) at various temperatures lower than the one at which CcdB denatures irreversibly. Changes in secondary structure at increasing urea concentrations (0–8 M) were followed by measuring the ellipticity at 225 nm in a 1 cm cuvette at the protein concentration of about 1 μ M.

3. Global Thermodynamic Analysis of Urea Unfolding Curves

The urea induced unfolding of CcdB from the dimeric native state (N_2) to the denatured monomeric state (D) may be described as a reversible two-state transition



The apparent equilibrium constant $K_{T,u}$ is a function of temperature (T) and urea concentration (u) and can be defined as:⁹

$$K_{T,u} = \frac{[D]^2}{[N_2]} = \frac{4(1-\alpha_{T,u})^2 c}{\alpha_{T,u}} \quad (2)$$

where $\alpha_{T,u}$ is the fraction of CcdB in the native state at given T and u , $\alpha_{T,u} = [N_2]/c$ where c is the total molar CcdB dimer concentration and $[N_2]$ and $[D]$ are molarities of N_2 and D, respectively. According to the model $c = [N_2] + [D]/2$ and the measured ellipticity ($\theta_{\lambda,T,u}$) at a given wavelength λ , T and u can be expressed in terms of the corresponding contributions $\theta_{N_2,\lambda,T,u}$ and $\theta_{D,\lambda,T,u}$ that characterize pure states N_2 and D as:

$$\theta_{\lambda,T,u} = \theta_{N_2,\lambda,T,u} \alpha_{T,u} + \theta_{D,\lambda,T,u} (1 - \alpha_{T,u}) \quad (3)$$

Since $\theta_{N_2,\lambda,T,u}$ and $\theta_{D,\lambda,T,u}$ can be estimated at any measured T as linear functions of u (pre- and post-transitional baselines; Figure 2b) the measured $\alpha_{T,u}$ can be expressed as (Figure 3)

$$\alpha_{T,u} = \frac{\theta_{\lambda,T,u} - \theta_{D,\lambda,T,u}}{\theta_{N_2,\lambda,T,u} - \theta_{D,\lambda,T,u}} \quad (4)$$

On the other hand, $\alpha_{T,u}$ can be connected to the thermodynamics of unfolding through the two-state transition model (equation 1) according to which the linear dependence of the standard Gibbs free energy of unfolding ($\Delta G_{T,u}^0$) on u can be at any T expressed as:

$$\Delta G_{T,u}^0 = \Delta G_T^0 - m \cdot u \quad (5)$$

where m is an empirical parameter correlated strongly to the amount of protein surface area exposed to the solvent upon denaturation¹⁰ and assumed to be temperature independent. ΔG_T^0 is the standard Gibbs free energy of unfolding in the absence of urea ($u = 0$) that may be expressed in terms of the corresponding standard Gibbs free energy ($\Delta G_{T_0}^0$) and standard enthalpy of unfolding ($\Delta H_{T_0}^0$) at a reference temperature $T_0 = 25$ °C and standard heat capacity of unfolding (ΔC_p^0) (assumed to be temperature independent) through the Gibbs-Helmholtz relation (integrated form):

$$\Delta G_T^0 = T \left\{ \frac{\Delta G_{T_0}^0}{T_0} + \Delta H_{T_0}^0 \left[\frac{1}{T} - \frac{1}{T_0} \right] + \Delta C_p^0 \left[1 - \frac{T_0}{T} - \ln \frac{T}{T_0} \right] \right\} \quad (6)$$

It follows from equations 5 and 6 that the model (adjustable) parameters $\Delta G_{T_0}^0$, $\Delta H_{T_0}^0$, ΔC_p^0 and m define, $\Delta G_{T,u}^0$ and also the corresponding $K_{T,u}^0$ ($K_{T,u}^0 = \exp(-\Delta G_{T,u}^0/RT)$). Consequently, the model function for $\alpha_{T,u}$ derived from equation 2 as:

$$\alpha_{T,u} = 1 + \frac{K_{T,u}}{8c} - \sqrt{\left(\frac{K_{T,u}}{8c} \right)^2 + \frac{K_{T,u}}{4c}} \quad (7)$$

can be compared to $\alpha_{T,u}$ values determined experimentally from equation 4. The values of adjustable parameters (Table 1) were obtained using the non-linear Levenberg–Marquardt regression procedure.¹¹ Then, the best global fit values of $\Delta G_{T_0}^0$, $\Delta H_{T_0}^0$ and ΔC_p^0 were used to estimate ΔG_T^0 (from equation 6), ΔH_T^0 from the Kirchhoff's law

$$\Delta H_T^0 = \Delta H_{T_0}^0 + \Delta C_p^0 (T - T_0) \quad (8)$$

and the corresponding entropy contribution, $T\Delta S_T^0$, from the general relation

$$\Delta G_T^0 = \Delta H_T^0 - T\Delta S_T^0 \quad (9)$$

The temperature dependences of ΔG_T^0 , ΔH_T^0 and $T\Delta S_T^0$ are presented in Figure 4.

4. Correlation Between Thermodynamic and Structural Parameters

Numerous recent studies on protein stability have shown that for protein unfolding both enthalpy of unfol-

ding (ΔH_T^0) and heat capacity of unfolding (ΔC_p^0) can be parameterized in terms of changes in solvent accessible polar (ΔA_p) and non-polar (ΔA_N) surface areas associated with the unfolding of the protein.^{10,12–15} Such a parameterization is based on the estimation of the non-polar (A_N) and polar (A_p) solvent accessible areas of proteins in the folded and unfolded states that were in the case of CcdB calculated with the program NACCESS version 2.1 using the probe size of 1.4 Å.¹⁶ A_N and A_p of native (folded) CcdB dimer were obtained from the known crystal structure³, while the A_N and A_p values of the completely unfolded CcdB monomers were estimated as the sum of the accessibilities of the protein residues located in the Ala-X-Ala tripeptides.^{12,13} The heat capacity (ΔC_p^0) and enthalpy of unfolding ($\Delta H_T^0 = \Delta H_{T_H}^0 + \Delta C_p^0(T - T_H)$) can be expressed as the sum of non-polar (subscript N) and polar (subscript P) contributions^{12–15}

$$\Delta C_p^0 = \Delta C_{p,N}^0 + \Delta C_{p,P}^0 = a\Delta A_N + b\Delta A_P \quad (10)$$

and

$$\begin{aligned} \Delta H_T^0 &= \Delta H_{T,N}^0 + \Delta H_{T,P}^0 \\ &= [c+a(T - T_H)]\Delta A_N + [d+b(T - T_H)]\Delta A_P \end{aligned} \quad (11)$$

Parameters $a = 1.88 \text{ J mol}^{-1} \text{ K}^{-1} \text{ \AA}^{-2}$, $b = -1.09 \text{ J mol}^{-1} \text{ K}^{-1} \text{ \AA}^{-2}$, $c = -35.3 \text{ J mol}^{-1} \text{ \AA}^{-2}$ and $d = 131.4 \text{ J mol}^{-1} \text{ \AA}^{-2}$ are obtained from Murphy and Freire¹² and Xie & Freire,¹⁷ while $\Delta H_{T_H}^0$ is parameterized as $\Delta H_{T_H}^0 = c\Delta A_N + d\Delta A_P$ ¹⁷ and represents the enthalpy of unfolding observed with most global proteins at their median transition temperature of $T_H = 60 \text{ }^\circ\text{C}$. The corresponding entropy of unfolding (ΔS_T^0) can be expressed as^{12–15,17,18}

$$\begin{aligned} \Delta S_T^0 &= \Delta S_{T,\text{solv}}^0 + \Delta S_{T,\text{other}}^0 = \\ &= \Delta S_{T,\text{solv}}^0 + \Delta S_{T,\text{conf}}^0 + \Delta S_{T,r+t}^0 \end{aligned} \quad (12)$$

The solvation contribution ($\Delta S_{T,\text{solv}}^0$) that describes the exposure of polar and non-polar groups to the solvent upon unfolding and dissociation of the CcdB dimer may be estimated as $\Delta S_{T,\text{solv}}^0 = \Delta C_p^0 \ln(T/T_S)$,^{12,19} where $T_S \approx 112 \text{ }^\circ\text{C}$ is the estimated reference temperature at which $\Delta S_{T,\text{solv}}^0$ is assumed to be equal to zero. The second term ($\Delta S_{T,\text{other}}^0$) can be considered as the sum of changes in configurational entropy ($\Delta S_{T,\text{conf}}^0$) and translational and rotational entropy ($\Delta S_{T,r+t}^0$) that accompany CcdB dimer unfolding and dissociation. $\Delta S_{T,\text{other}}^0$ was estimated by subtracting the calculated $\Delta S_{T,\text{solv}}^0 = \Delta C_p^0 \ln(T/T_S)$ from the corresponding measured ΔS_T^0 (equation 12; Figure 5). Moreover, $\Delta S_{T,r+t}^0$ can be estimated as an entropy change accompanying (rigid-body) dissociation of the dimer ($\Delta S_{T,r+t}^0 = 209 \text{ J K}^{-1} \text{ mol}^{-1}$)¹⁴ while $\Delta S_{T,\text{conf}}^0$ can be estimated as $\Delta S_{T,\text{conf}}^0 = \langle N \rangle 18 \text{ J K}^{-1} (\text{mol residue})^{-1}$ where $\langle N \rangle$ is the average number of amino-acid residues participating in the unfolding process and $18 \text{ J K}^{-1} (\text{mol residue})^{-1}$ is the average overall configu-

ration entropy change obtained from the thermodynamic database for unfolding of monomeric proteins.¹² As shown recently,^{20–24} the thermodynamics of a protein unfolding and some association processes can be correlated with its structural features through ΔA_N and ΔA_P values calculated from equations 10 and 11 using the experimentally obtained values for ΔC_p^0 and ΔH_T^0 . This enables the dissection of ΔC_p^0 and ΔH_T^0 into contributions due to interactions of non-polar ($\Delta C_{p,N}^0$, $\Delta H_{T,N}^0$) and polar ($\Delta C_{p,P}^0$, $\Delta H_{T,P}^0$) surfaces (see equations 10 and 11). Furthermore, the average number of the unfolded residues, $\langle N \rangle$, can be estimated as

$$\langle N \rangle = (\Delta A_N + \Delta A_P) \langle N \rangle_{\text{ST}} / (\Delta A_{N,\text{ST}} + \Delta A_{P,\text{ST}}) \quad (13)$$

where the $(\Delta A_N + \Delta A_P)$ term refers to the ΔA_N and ΔA_P values calculated from equations 10 and 11, the $(\Delta A_{N,\text{ST}} + \Delta A_{P,\text{ST}})$ term to those calculated for the complete unfolding from the structural data and $\langle N \rangle_{\text{ST}}$ is the total number of residues contained in the protein ($\langle N \rangle_{\text{ST}} = 202$). In addition, the estimation of $\langle N \rangle$ can be obtained also directly from equation 12 as:

$$\langle N \rangle = (\Delta S_T^0 - \Delta S_{T,\text{solv}}^0 - \Delta S_{T,r+t}^0) / 18 \text{ J K}^{-1} (\text{mol residue})^{-1} \quad (14)$$

5. Results and Discussion

The form of CcdB observed in a crystal is a homodimer (Figure 1) which is consistent with biophysical studies performed in solution.^{6,7} The two monomers fit tight-



Figure 1. Structure of the CcdB dimer in its native state. Ribbon representation of the crystal structure of the CcdB dimer³ was drawn using the program UCSF Chimera²⁵ and the coordinates from PDB ID 1vub. The non-polar and polar solvent accessible surface areas of the native dimer are estimated to be 5498 Å² and 4541 Å², respectively. The non-polar and polar solvent accessible surface areas of the two denatured CcdB monomers, calculated as the sum of the accessibilities of the CcdB residues located in the Ala-X-Ala tripeptides, are estimated to be 19676 Å² and 13732 Å², respectively. The amino acid composition of each CcdB monomer consisting of 101 residues is as follows: MQFKVYTYKR ESRYRLFVDV QSDIIDTPGR RMVIPLASAR LLSDKVSREL YPVVHIGDES WRMMTTDMAS VPVSVIGEEV ADLSHRENDI KNAINLMFWG I.

ly onto each other, mainly due to van der Waals interactions between the side chains. This is reflected in about 2500 Å² of surface area buried upon dimer formation of which 1600 Å² comes from hydrophobic side-chain contacts.⁵

Thermal denaturation monitored by CD spectroscopy (Figure 2a) indicates that the CcdB dimer is thermally highly stable and that its thermal denaturation is an irreversible process (Figure 2a) accompanied by a visible precipitation of the protein. On the other hand, CD spectroscopy shows (Figure 2b) that the urea-induced denaturation at temperatures between 5 and 40 °C may be considered as a reversible process. Urea induced unfolding curves measured by CD spectroscopy at a single wavelength and given temperature (Figure 2b) and transformed into the dependence of the fraction of CcdB in the native dimeric state, $\alpha_{T,u}$, on urea concentration, u (equation 4) are presented in Figure 3.

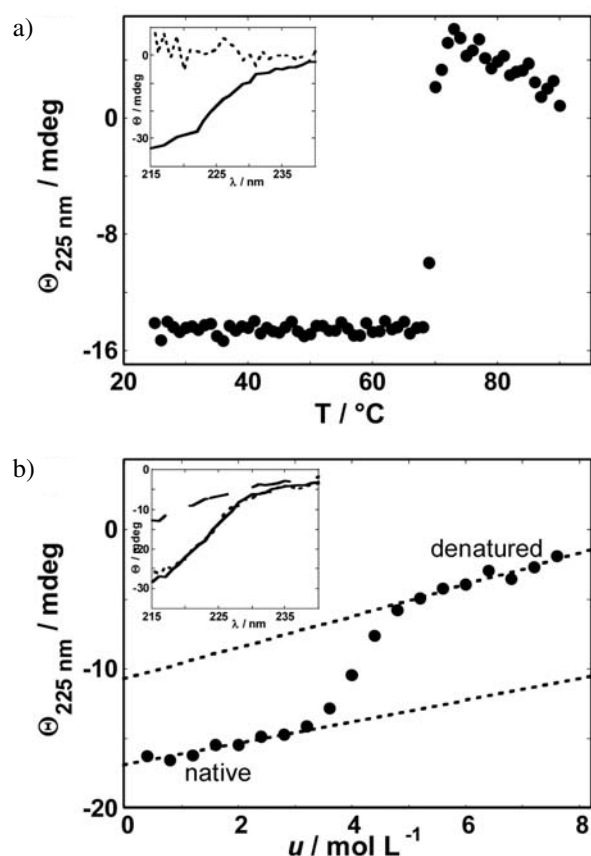


Figure 2. Thermal and urea induced denaturation of CcdB monitored by spectropolarimetry. (a) Thermal denaturation profile and the corresponding spectra (inset) measured at 25 °C before (full line) and after heating to 90 °C (dotted line); (b) Urea denaturation profile measured at 5 °C. Pre- and post-translational baselines (dotted lines) define ellipticities of the native and denatured state over the whole range of urea concentrations, u (see equation 4). Inset represents spectra measured at $u = 3.5$ M (full line), 7.0 M (disconnected line) and at 3.5 M (dotted line; after dilution from 7.0 M and corresponding multiplication of spectra by the dilution factor) indicating high degree of reversibility of urea denaturation.

Global fitting of the reversible two-state model function (equation 7) shows good agreement with experimental $\alpha_{T,u}$ versus u curves measured at various temperatures (Figure 3). The resulting best-fit thermodynamic parameters $\Delta G_{T_0}^o$, $\Delta H_{T_0}^o$, ΔC_p^o are in relatively good agreement with the corresponding literature values (Table 1).

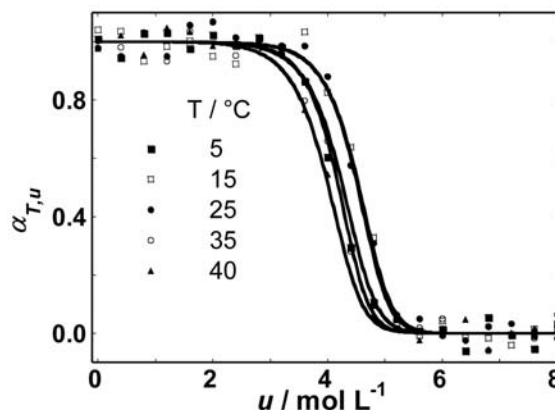


Figure 3. Global model analysis of urea induced denaturation profiles. The measured fraction of native CcdB dimer (points; see equation 4) and the corresponding best global fit of the two-state model function (lines; see equation 7). The best fit parameters are presented in Table 1.

The thermodynamic profiles of CcdB unfolding estimated from the best-fit parameters (Table 1) are presented in Figure 4. The observation that CcdB folding in the standard state at physiological temperatures is an enthalpy driven process, accompanied by a negative entropy contribution and negative heat capacity change is a general feature of globular proteins.¹³ More interesting is the dissection of the measured thermodynamic parameters of unfolding at 25 °C to various contributions based on equations 10 – 12 (Figure 5). Parsing of enthalpic contribution indicates that the contribution due to the changed interactions of polar surfaces that favor folding overcompensates the corresponding contributions of non-polar surfaces that on average favor unfolding. Furthermore, parsing of entropic contributions indicates that the contribution due to the changes of configurational, translational and rotational freedom ($\Delta S_{T,other}^o$) that favors unfolding slightly prevails over the solvation contribution ($\Delta S_{T,solv}^o$) which favors CcdB folding.

As shown recently,^{20,21} the correlation of the experimentally determined thermodynamics of protein unfolding with its structural features can be carried out using an approach in which ΔA_N , ΔA_p and $\langle N \rangle$ that accompany unfolding and dissociation of CcdB dimer are calculated from combination of experimental thermodynamic data and parametrized equations 10 and 11. These calculations show that upon urea denaturation of CcdB both $\Delta A_N/\Delta A_{N,ST}$ and $\Delta A_p/\Delta A_{p,ST}$ ratios are about 70%. Similarly, the $\langle N \rangle/\langle N \rangle_{ST}$ in which $\langle N \rangle$ is determined either from

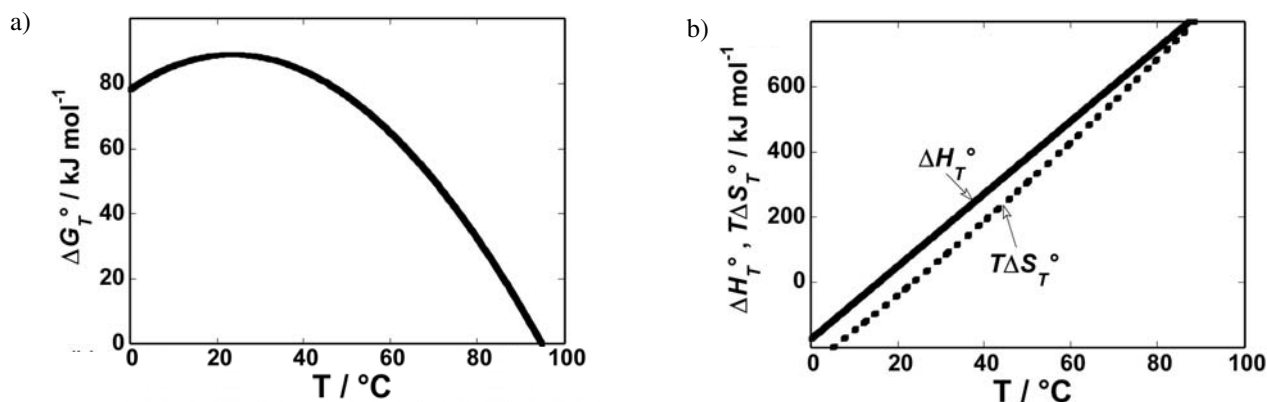


Figure 4. Thermodynamic profile of CcdB unfolding. (a) Standard Gibbs free energy, ΔG_T^0 ; (b) enthalpy, ΔH_T^0 (full line), and entropy contribution, $T\Delta S_T^0$ (dotted line) in the absence of urea ($u = 0$) as functions of temperature, T , were estimated from the best-fit parameters (Table 1) by using equations 6, 8 and 9.

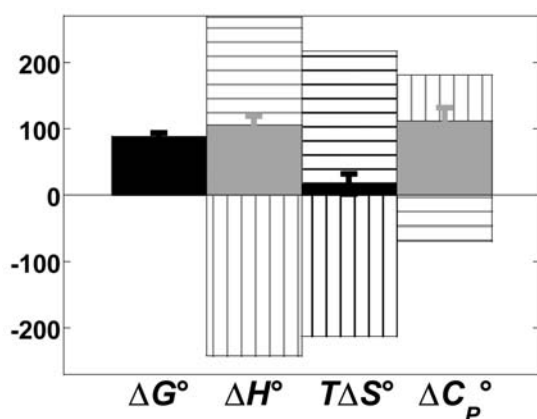


Figure 5. Thermodynamic profile of CcdB unfolding at $T = 25$ °C. The standard thermodynamic quantities ΔG_T^0 (black), ΔH_T^0 (grey), $T\Delta S_T^0$ (black) are presented in $\text{kJ mol}_{\text{dimer}}^{-1}$, while for clarity reasons ΔC_p^0 (grey) is presented in $10 \text{ kJ mol}_{\text{dimer}}^{-1} \text{ K}^{-1}$. Contributions to ΔH_T^0 due to the changed interactions of polar (hatched horizontally) and non-polar surfaces (hatched vertically). $T\Delta S_T^0$ contributions due to the differences in solvation of the folded and unfolded state (hatched vertically) and other contributions that contain changes of conformational, translational and rotational freedom upon unfolding (hatched horizontally). Contributions to ΔC_p^0 due to the exposure of polar (hatched horizontally) and non-polar (hatched vertically) surfaces. For clarity, the estimated ΔH_T^0 and $T\Delta S_T^0$ contributions (see equations 10–12) are divided by a factor of four.

equation 13 ($\langle N \rangle = 140$) or 14 ($\langle N \rangle = 150$) is about 70%. Evidently, these $\Delta A_N / \Delta A_{N,ST}$, $\Delta A_P / \Delta A_{P,ST}$ and $\langle N \rangle / \langle N \rangle_{ST}$ values show that the degree of urea induced unfolding is significantly lower than unity. The resulting conclusion is that the urea-denatured state is not a completely unfolded state which is in accordance with our far-UV CD results (Figure 2). Moreover, reasonable agreement between the $\langle N \rangle$ values determined from two different relations (equations 13 and 14) suggests that the presented enthalpy and entropy contributions have a real physical meaning. We are well aware that these contributions determined from the described combination of experimental thermodynamics and structure-based parameterization can be con-

sidered only as reasonably good approximations since they comprise errors of the empirical parameterization and those of the measured thermodynamic quantities. Nevertheless, we believe that using this approach one can explain, at least in a semi-quantitative way, the correlation between the thermodynamics of urea-induced unfolding of its and the structural features of CcdB folded and unfolded state.

Table 1. Comparison of the thermodynamic parameters of CcdB unfolding at $T_0 = 25$ °C obtained from global fitting of the model function (equation 7)^a to the chemical unfolding data (Figure 3) with the corresponding parameters obtained from other thermodynamic studies^{6,7}

denaturant	$\Delta G_{T_0}^0 / \text{kJ mol}^{-1}$	$\Delta H_{T_0}^0 / \text{kJ mol}^{-1}$	$\Delta C_p^0 / \text{kJ mol}^{-1} \text{ K}^{-1}$
urea (this work)	89	105	11
GdmHCl (reference 6)	87	166	13
GdmHCl (reference 7)	85	31	12

^aThe parameter errors are estimated to be about $\pm 5\%$ for $\Delta G_{T_0}^0$, $\pm 15\%$ for $\Delta H_{T_0}^0$ and $\pm 10\%$ for ΔC_p^0 . Our model analysis resulted in the best-fit value of parameter m (equation 5) of $12.6 (\pm 1.3) \text{ kJ mol}^{-1} \text{ M}^{-1}$

6. Acknowledgment

We thank Prof. R. Loris for providing the purified toxin CcdB used in this work that was supported by the Ministry of Higher Education, Science and Technology and by the Agency for Research of Republic of Slovenia through the Grants No. P1-0201 and J1-6653.

7. References

1. L. Buts, J. Lah, M.-H. Dao-Thi, L. Wyns, R. Loris, *Trends Biochem. Sci.* **2005**, *30*, 672–679.
2. P. Bernard, M. Couturier, *Mol. Biol.* **1992**, *226*, 735–745.
3. T. Miki, J. A. Park, K. Nagao, N. Murayama, T. Horiuchi, *J. Mol. Biol.* **1992**, *225*, 39–52.

4. M.-H. Dao-Thi, L. Van Melderen, E. De Genst, H. Afif, L. Wyns, R. Loris, *J. Mol. Biol.* **2005**, *348*, 1091–1102.
5. R. Loris, M.-H. Dao-Thi, E. M. Bahassi, L. Van Melderen, F. Poortmans, R. Liddington, M. Couturier, L. Wyns, *J. Mol. Biol.* **1999**, *285*, 1667–1677.
6. M.-H. Dao-Thi, J. Messens, L. Wyns, J. Backmann, *J. Mol. Biol.* **2000**, *299*, 1373–1386.
7. K. Bajaj, G. Chakshusmathi, K. Bachhawat-Sikder, A. Surolia, R. Varadarajan, *Biochem J.* **2004**, *380*, 409–417.
8. S. C. Gill, P. H. von Hippel, *Anal. Biochem.* **1989**, *182*, 319–326.
9. I. Drobnak, M. Seručnik, J. Lah and G. Vesnaver, *Acta Chim. Slov.* **2007**, *54*, 445–451.
10. J. K. Myers, N. C. Pace, M. J. Scholtz, *Protein Sci.* **1995**, *4*, 2138–2148.
11. W. H. Press, B. P. Flannery, S. A. Teukolsky, W. T. Vetterling, *Numerical Recipes* **1992** Cambridge University Press, Oxford.
12. K. P. Murphy and E. Freire, *Adv. Protein Chem.* **1992**, *43*, 313–361.
13. G. I. Makhatadze, P. L. Privalov, *Adv. Protein Chem.* **1995**, *47*, 307–425.
14. R. S. Spolar, M. T. Jr. Record, *Science* **1994**, *263*, 777–784.
15. A. D. Robertson, K. P. Murphy, *Chemical Reviews* **1997**, *97*, 1251–1267.
16. S. J. Hubbard, and J. M. Thornton, *NACCESS computer program* **1993**, University College London.
17. D. Xie, E. Freire, *Proteins Struct. Funct. Genet.* **1994**, *19*, 291–301.
18. K. H. Lee, D. Xie, E. Freire, L. M. Amzel, *Proteins Struct. Funct. Genet.* **1994**, *20*, 68–84.
19. R. L. Baldwin, *Proc. Natl. Acad. Sci. USA* **1986**, *83*, 8069–8072.
20. J. Lah, M. Šimič, G. Vesnaver, I. Marianovsky, G. Glaser, H. Engelberg-Kulka and R. Loris, *J. Biol. Chem.* **2005**, *280*, 17397–17407.
21. J. Lah, I. Prisljan, B. Kržan, M. Salobir, A. Francky and G. Vesnaver, *Biochemistry* **2005**, *44*, 13883–13892.
22. J. Lah, I. Marianovsky, G. Glaser, H. Engelberg-Kulka, J. Kinne, L. Wyns and R. Loris, *J. Biol. Chem.* **2003**, *278*, 14101–14111.
23. J. Lah, M. Bešter-Rogač, T.-M. Perger, G. Vesnaver, G. J. *Phys. Chem. B* **2006**, *110*, 23279–26291.
24. J. Lah, I. Drobnak, M. Dolinar, G. Vesnaver, *Nucleic Acids Res.* **2008**, *36*, 897–904.
25. E. F. Pettersen, T. D. Goddard, C. C. Huang, G. S. Couch, D. M. Greenblatt, E. C. Meng, and T. E. Ferrin, *J. Comput. Chem.* **2004**, *25*, 1605–1612.

Povzetek

Operon *ccd* iz *E. coli* kodira antitoksin CcdA in toksin CcdB ter predstavlja t.i. modul toksin-antitoksin. Če CcdA in CcdB nista medsebojno povezana v kompleks, prosti CcdB napade celično tarčo, DNA girazo, in z inhibicijo prepisovanja in podvajanja DNA povzroči smrt bakterijske celice. Pri fizioloških pogojih CcdB obstaja kot homodimer. Za razliko od nedavno raziskanega razvitja CcdB, se v naši študiji osredotočamo na povezavo med strukturo in termodinamiko denaturacije, ki je potrebna za razumevanje stabilnosti in delovanja CcdB na molekularnem nivoju. V tej luči so bili termodinamski parametri razvitja dobljeni s pomočjo globalne analize denaturacijskih krivulj merjenih pri različnih temperaturah s spektropolarimetrijo. Razčlenjeni so bili na prispevke, ki izhajajo iz razlik v intra- in inter-molekularnih interakcijah, ki jih CcdB lahko tvori v zvitem dimerem in razvitem monomernem stanju. Ta razčlemba pokaže, da razviti monomeri ohranijo približno 30 % strukture, kar pomeni, da opaženo denaturirano stanje doseženo z visoko koncentracijo uree ne ustreza popolnoma razvitemu stanju proteina.